



Ultra-wideband and Multifunctional Metamaterial Polarization Rotator in Terahertz Band

Xiang Miao^{1,2} · Zhongyin Xiao^{1,2} · Zhentao Cui^{1,2} · Tiantian Zheng^{1,2} · Xiaoyu Wang^{1,2}

Received: 3 November 2021 / Accepted: 22 March 2022 / Published online: 29 April 2022
© The Author(s), under exclusive licence to Springer Science+Business Media, LLC, part of Springer Nature 2022

Abstract

In this paper, a reflective polarization convertor is proposed based on a sandwich structure consisting of an “I”-shaped resonator at the top, a medium layer of foam, and a metal layer at the bottom. The characteristics of ultra-wideband (UWB) and higher relative bandwidth (RB) have been achieved than previous structures. The structure effectively controls the polarization of electromagnetic waves in the terahertz band, which convert the incident linear-polarized (LP) wave to cross-polarized wave within 2.75–10.35THz, with a relative bandwidth of 116% and a polarization conversion ratio (PCR) greater than 90%. In addition, this structure also converts the incident linear-polarized wave to circular-polarized wave in the range of 2.28–2.65THz with axial ratio (AR) less than 3 dB. The characteristics are also analyzed based on the surface current distribution. The reason of realizing UWB polarization conversion is explained by polarization decomposition method. Our structure could provide many potential applications in radar antenna, metamaterial lens, and other electromagnetic wave and optical fields.

Keywords Ultra-wideband · Polarization converter · Terahertz · “I”-shaped resonator

Introduction

Polarization is an important characteristic of an electromagnetic wave, which refers to the oscillation direction of the electric field in a plane perpendicular to the propagation direction [1]. Since there are many phenomena which have certain requirements on the polarization mode of the electromagnetic wave, how to effectively control and manipulate the polarization state of an electromagnetic wave has aroused the interest of many researchers. Traditional polarization conversion devices are usually realized by birefringence crystals with a huge volume, which requires the accumulation of the required phase difference, resulting in the increase of device miniaturization research. In recent years, the emergence of electromagnetic metamaterials has realized

the increasing need for miniaturization of traditional materials. Electromagnetic metamaterials are synthetic, that is, nonexistent in nature, materials, or structures that periodically depend on the size of the subwavelength. Its important characteristic is a unit to simulate the traditional materials of atomic structure. It is subwavelength structure, make it have unique properties including negative permittivity, negative magnetic permeability and negative index. There exists a plenty of important applications in radar antenna [2], metamaterial lens [3], perfect absorber [4, 5], electromagnetic induced transparency (EIT) devices [6–9], and many other fields. Therefore, it is of great significance to design a device to control the polarization state of electromagnetic waves by using metamaterials.

There are two kinds of metamaterial structures to realize polarization conversion, which are transmission and reflection polarization converters. Transmission polarization converters are usually divided into birefringence based on anisotropic metamaterials [10, 11] and optical properties based on chiral metamaterials [12, 13]. In the reflective polarization converter, recently, several structures have been designed as a metasurface. In 2017, a high-efficiency and wide-bandwidth linear polarization converter using double *U*-shaped metasurface was

✉ Zhongyin Xiao
zhyxiao@shu.edu.cn

¹ School of Communication and Information Engineering, Key Laboratory of Specialty Fiber Optics and Optical Access Networks, Shanghai University, Shanghai, China

² School of Communication and Information Engineering, Shanghai Institute for Advanced Communication and Data Science, Shanghai University, Shanghai, China

proposed by Mei Z et al. [14]. The design is based on the two-dimensional artificial electromagnetic materials and micro-antenna array. The conversion bandwidth is 6.91–14.31 GHz. A polarization converter formed from the planar anisotropic metamaterial (MM) using cut-wire (CW) structure was proposed by Zhao J et al. [15] to realize that PCR is above 90% in the frequency range of 5.1–12.1 GHz and the relative bandwidth is up to 78.6%. Many of the metasurfaces designed with this structure achieve broadband characteristics. Some structures achieve dual-band [16] and multi-band polarization conversion effect [17]. In 2020, a reflective polarization converter was designed based on coding topology by Qi Y et al. by encoding and adjusting the Pancharatnam-Berry (PB) phase to achieve a broadband polarization conversion with relative bandwidth of 89% [18]. There are other similar designs based on encoding and adjusting the Pancharatnam-Berry (PB) phase [19]. There also exist several designs which have a multi-layer structure made of a variety of different metasurface structures to obtain a broadband polarization conversion by adding multiple resonators artificially [20]. However, the multi-layer structures increase the complexity of fabrication and face the problems of low efficiency. Unfortunately, few polarization converters have a relative bandwidth of more than 110% to realize UWB polarization conversion.

In this paper, a UWB multifunctional metamaterial structure is proposed, and a UWB linear polarization converter with wider working bandwidth is obtained, and different functions are realized in different frequency bands. The proposed polarization converter converts the incident linear-polarized wave to cross-polarized wave within 2.75–10.35THz, with 116% relative bandwidth and PCR over 90%, which has the characteristics of ultra-wideband and higher relative bandwidth than previous structures. The linear-polarized wave is also converted into circular-polarized wave in the frequency range of 2.28–2.65THz with axial ratio less than 3 dB.

Models and Simulations

Figure 1 shows a schematic diagram of the proposed structure, consisting of three parts, the top “I”-shaped resonator, the middle air layer, and the bottom continuous metal plate. The material of the top “I”-shaped metal resonator and the bottom metal plate is copper, and the thickness t is $0.03 \mu\text{m}$. The middle layer in the middle is the air layer, and the relative dielectric constant is set as 1.0. Foam materials similar to the dielectric properties of air may also be considered, making the structure simple and easy to manufacture. The polymethacrylimide (PMI) foam material has a dielectric constant ϵ_r of 1.05, which meets $\epsilon_r \approx 1$, and its relative permeability $\mu_r \approx 1$; its properties are very similar to air [21]. Therefore, it can be selected as the supporting dielectric material without affecting the electromagnetic characteristics of the structure. The size of the top metal resonator is continuously optimized by simulation, and the metal corner point is tangent to the boundary of the device element. After optimization, detailed geometric parameters of the unit structure are shown in Fig. 1b. Specific structural parameters are as follows: $p = 30 \mu\text{m}$, $l = 24.5 \mu\text{m}$, $d = 11 \mu\text{m}$, $w = 4.75 \mu\text{m}$, $t_1 = 1 \mu\text{m}$.

Taking the y -polarized wave as an example, the definition equation of the co-polarized reflection coefficient is expressed as $r_{yy} = |E_{yr}| / |E_{yi}|$, where $|E_{yr}|$ represents the component of the reflected electric field in the y -direction, and $|E_{yi}|$ represents the component of the reflected electric field in the x -direction. The definition equation of cross-polarized reflection coefficient is expressed as $r_{xy} = |E_{xr}| / |E_{yi}|$, where $|E_{xr}|$ represents the amplitude of the reflected electric field in the x -direction.

PCR is usually used to evaluate the efficiency of polarization converters, defined by the formula $PCR = |r_{xy}|^2 / (|r_{xy}|^2 + |r_{yy}|^2)$. Metamaterials are synthetic materials with periodic or aperiodic structures arranged in subwavelength units. The

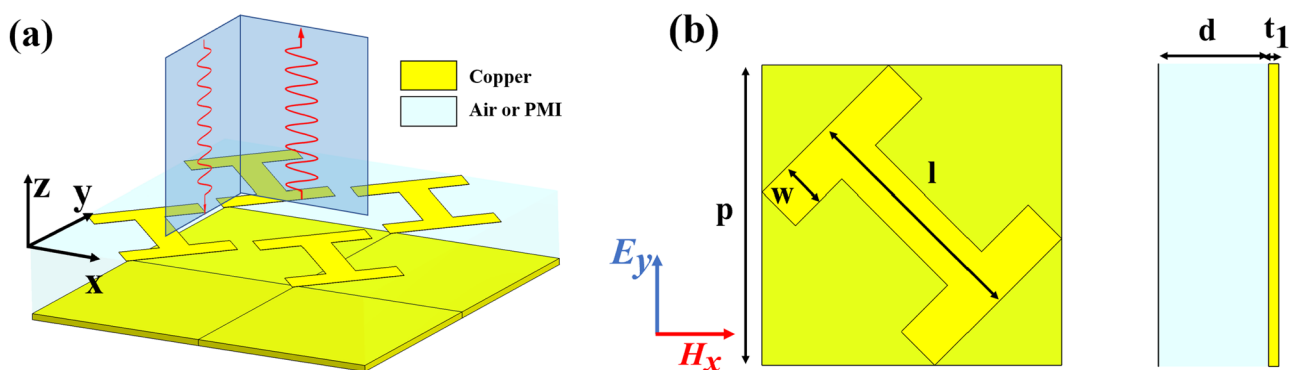


Fig. 1 Structure: **a** 3D view, **b** front view and side view

metamaterials proposed in this paper are periodic structures. Therefore, in the simulation of commercial software CST Studio Suite, it is necessary to set the structure to form periodic arrangement structure in the way of unit cell in the *x*-axis and *y*-axis directions, and then set open (add space) in the *z*-axis direction to achieve normal or oblique incidence at a certain distance, and finally start the numerical simulation.

The simulation results of the structure are shown in Fig. 2. From Fig. 2b, it can be seen that the PCR results are above 90% in the frequency range of 2.75–10.35THz. We define the bandwidth $\Delta f = f_H - f_L$ and center frequency $f_0 = (f_H + f_L)/2$, where f_h and f_l represent the upper and lower cutoff frequencies of the operating bandwidth respectively. Therefore, the calculation formula of relative bandwidth is $RB = \Delta f / f_0$.

The calculation results show that the structure can obtain a relative bandwidth of 116% (PCR > 90%), which is higher than the previous structure. In addition, compared with other existing polarization converters, the structure has higher relative bandwidth and simpler geometry. Table 1 shows comparisons between other reported reflective polarization converters. It can be seen from the table that the proposed structure realizes high-efficiency polarization conversion in broadband.

Table 1 Comparison with other broadband terahertz band polarization converters

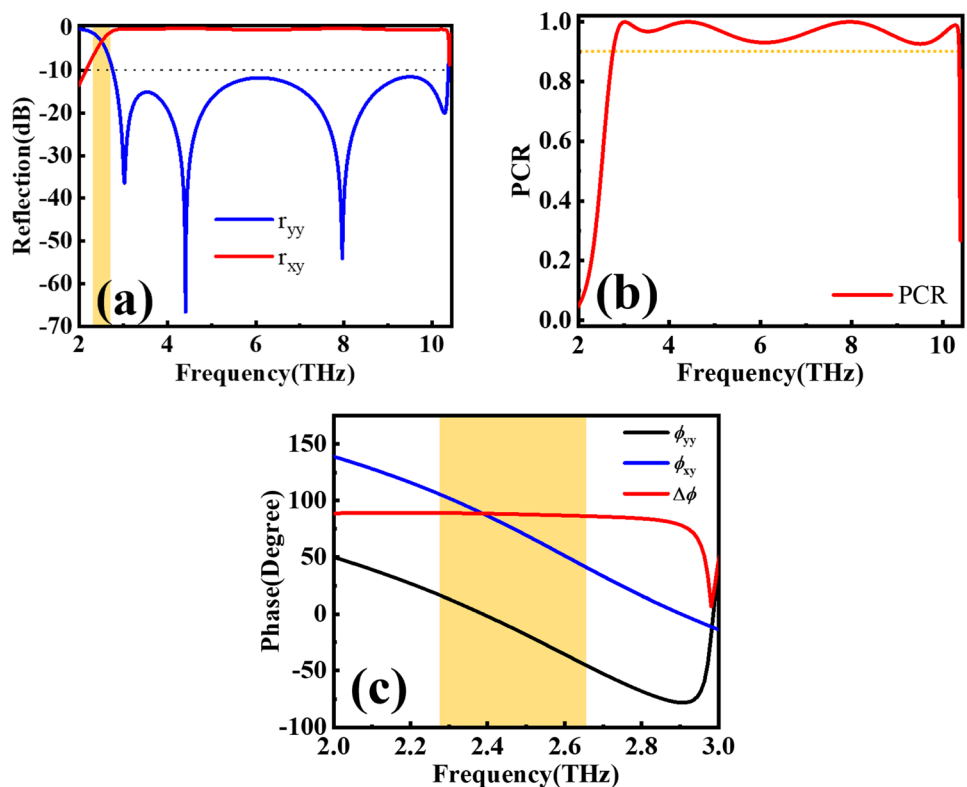
Works	OB ^a (THz)	RB ^b (%)
Ref. [23]	0.91–1.67	58.9
Ref. [22]	2.10–5.03	82.2
Ref. [24]	0.55–1.37	85.4
Ref. [18]	2.04–5.33	89
Ref. [25]	0.65–1.92	103
This paper	2.75–10.35	116

^aOperating bandwidth (PCR > 90%)

^brelative bandwidth (PCR > 90%)

In addition, it can be observed from Fig. 2a and c that in the range of 2.28–2.65THz, the difference between the magnitude of the cross-polarized reflection coefficient and the co-polarized reflection coefficient is less than 3 dB, and the phase difference between the cross-polarized reflection coefficient and the co-polarized reflection coefficient is about 90° within this frequency range. Figure 2c shows the area shaded. Therefore, the conversion from linear-polarized to circular-polarized is achieved in the frequency range of 2.28–2.65THz.

Fig. 2 **a** The reflection coefficient of the incident y-polarized wave, **b** PCR, **c** the phase of the co-polarized reflection coefficient and the cross-polarized reflection coefficient and the phase difference between them. The shaded areas in (a) and (c) indicate that the amplitude and phase characteristics of the current reflected wave in this frequency band meet the conditions for forming circular-polarized waves respectively



Discussion

In order to analyze the polarization conversion performance of the structure, the finite element method is used to simulate the structure. Since the structure is distributed symmetrically after rotating 45°, the same polarization conversion effect can be obtained if the direction of the electric field of the incident wave is in the x -direction or the y -direction. From basic electromagnetic theory, it is known that the phase difference between two orthogonal components of a linear-polarized wave is 0° or 180°. If the electric field vector of the electromagnetic wave which is incident vertically along the metasurface is decomposed along the direction of the orthogonal coordinate axis, and if the reflection amplitude of the same polarization of the two orthogonal components is the same and the phase difference is 180°, then the phase mutation of 90° can be realized in the synthetic wave. The working principle of the polarization converter is shown in Fig. 3a. The coordinate axis uOv is rotated by 45° from the coordinate axis xOy . As mentioned above, the same polarization conversion effect is obtained regardless of whether the electric field direction of the incident wave is in the x -direction or the y -direction. Therefore, taking the incident y -polarized wave as an example, the incident wave is expressed as

$$\vec{E}_i = E_i e^{jkz} \hat{y} = \frac{\sqrt{2}}{2} (E_{iu} \hat{u} + E_{iv} \hat{v}) e^{jkz} \tag{1}$$

Reflected waves are represented by reflected waves along the u and v axes

$$\vec{E}_r = \frac{\sqrt{2}}{2} \left[(r_{uu} E_{iu} e^{-jkz + \phi_{uu}} + r_{uv} E_{iv} e^{-jkz + \phi_{uv}}) \hat{u} + (r_{vu} E_{iu} e^{-jkz + \phi_{vu}} + r_{vv} E_{iv} e^{-jkz + \phi_{vv}}) \hat{v} \right] \tag{2}$$

In this formula, r_{uu} , r_{uv} , r_{vv} , and r_{vu} represent respectively the co-polarized and cross-polarized reflection coefficients in the coordinate system and ϕ_{uu} , ϕ_{uv} , ϕ_{vv} , and

ϕ_{vu} represent respectively the phase of co-polarized and cross-polarized reflection in the coordinate system.

According to the electric field vector operation rule, when the conditions are satisfied,

$$\begin{cases} r_{uu} = r_{vv} = r \\ r_{vu} - r_{uv} = 0 \\ \Delta\phi = \phi_{vv} - \phi_{uu} = \pi + 2k\pi \end{cases} \tag{3}$$

The reflection wave is expressed as

$$\vec{E}_r = \frac{\sqrt{2}}{2} (r_{uu} E_{iu} e^{j(-kz + \phi_{uu})} \hat{u} + r_{vv} E_{iv} e^{j(-kz + \phi_{vv} + \pi)} \hat{v}) = r E_i e^{j(-kz + \phi_{uu})} \hat{x} \tag{4}$$

Therefore, the incident y -polarized wave can be rotated into x -polarized wave after reflection, so the structure of the resonant layer needs to be linear symmetric with respect to u and v axes.

As can be seen from Fig. 3a and b, within the frequency range from 2.75 to 10.35THz, the reflected amplitude of the electric field component in the u direction r_{uu} and the electric field component in the v direction r_{vv} are both close to 1, and their phase difference is about 180°. Therefore, the ultra-wideband efficient polarization conversion is realized. At some frequency points, especially at 3.013THz, 4.344THz, 7.974THz, and 10.273THz, the phase difference is close to 180°.

In order to understand the physical mechanism of the polarization converter, the surface current distribution at the four resonant frequencies of 3.013THz, 4.344THz, 7.974THz, and 10.273THz is obtained by simulation, as shown in Fig. 4. When electromagnetic wave is incident to

the metal boundary, the metal surface free electrons oscillate. If the electron oscillates at a frequency consistent with that of the incident wave, it resonates, then the resonance

Fig. 3 a The principle of polarization conversion. b The reflection coefficient and phase difference of the incident wave along the u -axis and v -axis in the direction of the electric field

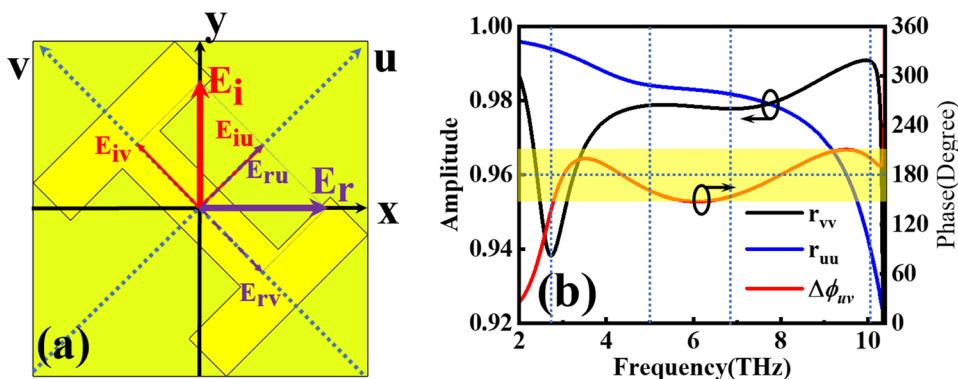
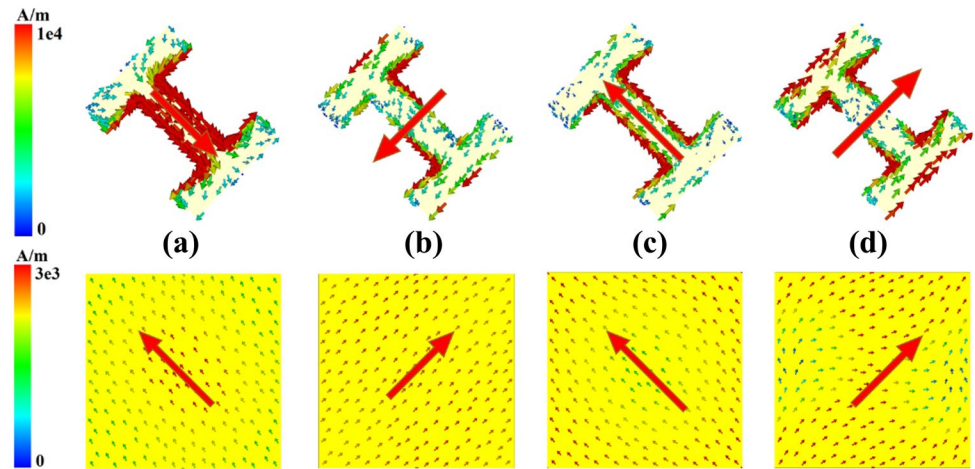


Fig. 4 Surface current distribution of the structure at different resonant frequencies: **a** 3.013THz, **b** 4.344THz, **c** 7.974THz, **d** 10.273THz

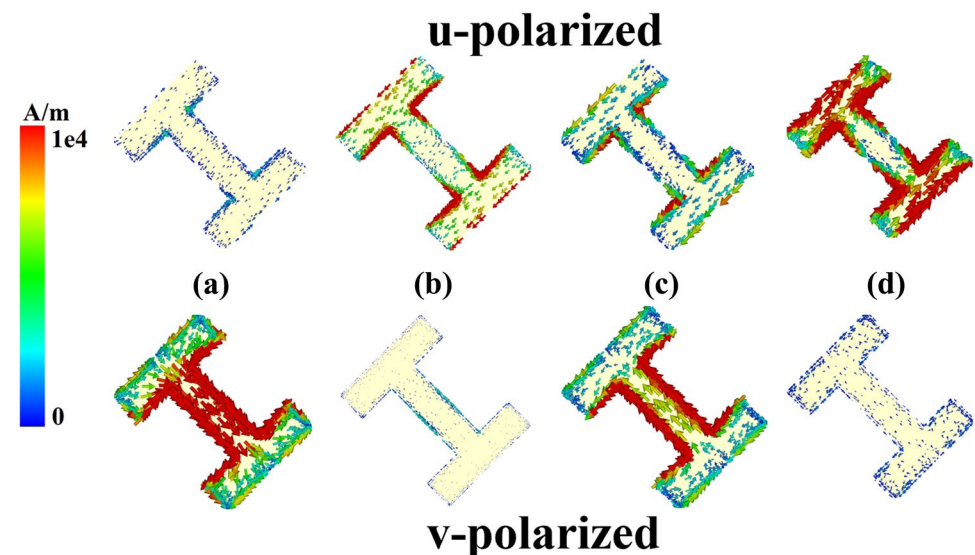


state of the electric field transforms the free energy of the metal surface into vibration. This is plasma resonance on a metal surface. It can be seen that at 3.013THz and 4.344THz, the resonator surface current is anti-parallel to the current on the metal plate. Therefore, the single current loop formed in the middle layer is the first-order magnetic resonance, and at 7.974THz and 10.273THz, the resonator surface current is parallel to the current on the metal plate, corresponding to the first-order electric resonance. This is because magnetic dipoles produce circular currents, while electrical dipoles produce directional currents. It is precisely because the combination of four resonances with overlapping regions guarantees the broadband performance of the designed polarization converter.

In addition, it can also be analyzed from u and v polarization decomposition [26]. Through detailed observation, it is found that r_{uu} and r_{vv} each have minor values at two frequencies near the resonant frequencies of these four PCR peaks,

which are 5.02THz, 10.11THz, 2.73THz, and 6.88THz respectively, as shown in Fig. 3b. Simulation results show that they are excited by u - and v -polarized waves respectively in Fig. 5. Dielectric losses occur at these four frequencies. Since the structure is symmetric for both u -axis and v -axis, the surface current distribution of the eigenmode excited by the u -polarized wave and v -polarized wave is completely symmetric with respect to the u -axis and v -axis, and cross-polarization does not occur. As shown in Fig. 5a, at frequency 2.73THz, when incident with v -polarized wave, it can excite the middle part of “I”-shaped resonator parallel to the v -axis direction, and the current mostly concentrates on the metal surface. This frequency is also the first eigenfrequency of v -polarized wave resonance on this structure. However, compared with the situation of that v -polarized incident wave, in the direction parallel to the u -axis, it cannot be excited by u -polarized incident wave. The reason is that at 2.73THz, the reflection of v -polarized wave has

Fig. 5 Surface current distribution of the structure with u - and v -polarized wave at different frequencies: **a** 2.73THz, **b** 5.02THz, **c** 6.88THz, **d** 10.11THz



a minimum value, while that of u -polarized wave has no minimum value, which indicates that at this frequency, the main resonance is caused by v -polarized wave. When the frequency is 5.02 THz, v -polarized incident wave cannot excite the part of “T”-shaped resonance parallel to the v -axis in Fig. 5(b). When a u -polarized wave is incident, a resonance effect occurs in the direction parallel to the u -axis. This method of analysis can be used to explain the similar cases at 6.88THz and 10.11THz frequencies. However, these frequency points are not the frequency points where the PCR reaches maximum. The reason is that these circumstances do not satisfy the phase condition in Eq. (3). The phase of these frequency points is shown in Fig. 3b. As shown in Fig. 6, the surface currents at 3.013THz, 4.344THz, 7.974THz, and 10.273THz are simulated respectively. It can be seen that the PCR peak at each resonant frequency point is the result of u -polarized wave, v -polarized wave, and phase interaction.

It is very important to study the angle dependence of reflective polarization converters. Figure 7 shows the effect of PCR with the change of frequency and incident angle. It can be seen that the bandwidth of the polarization converter decreases with the increase of incident angle. This is usually attributed to surface destructive interference at oblique incidence. At higher frequencies, the influence of the incident angle on the destructive interference increases.

When the operating frequency is in the range of 2.28–2.65THz, this structure can convert the linear-polarized incident wave into the circular-polarized reflected wave.

The conditions for the realization of linear-to-circular-polarized electromagnetic waves are $\Delta\phi = \phi_x - \phi_y = \pm\frac{\pi}{2}$ and $E_{xm} = E_{ym} = E_m$. As can be seen from Fig. 2a and c, the difference between the magnitudes of the cross-polarized reflection coefficient and the co-polarized reflection coefficient is less than 3 dB, and within this frequency range, the phase

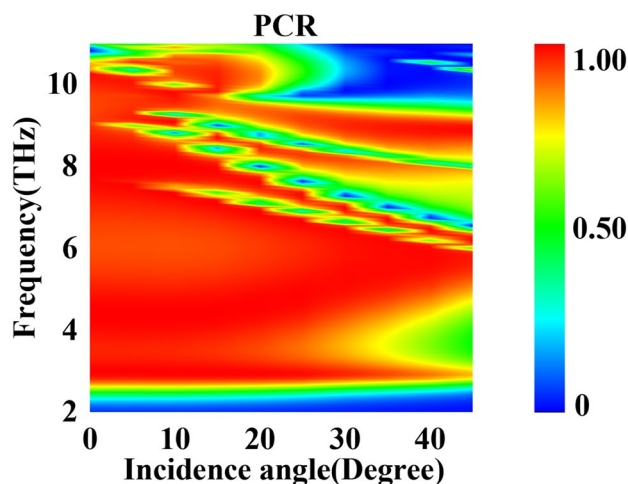


Fig. 7 Effects of different incidence angles and frequencies on PCR

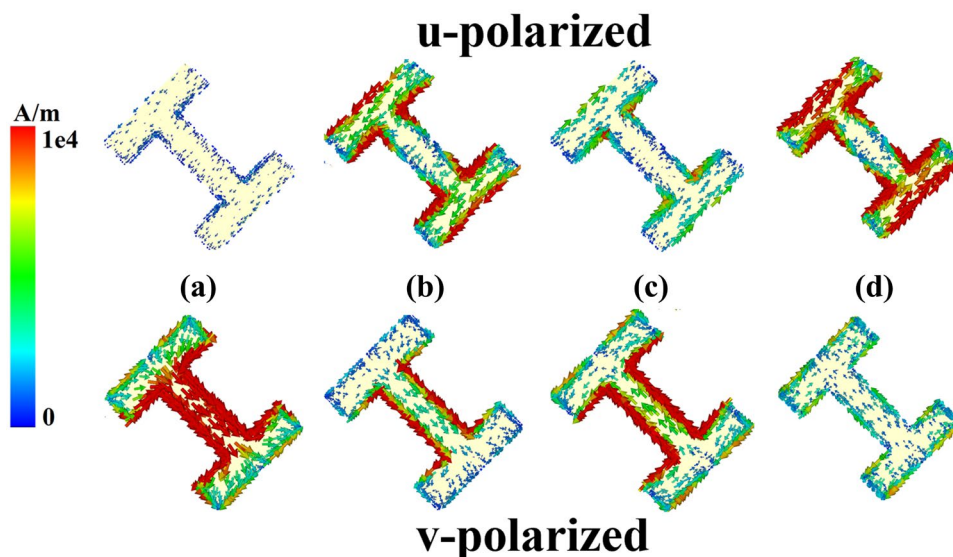
difference between the cross-polarized reflection coefficient and the co-polarized reflection coefficient is about 90° , which satisfies the conditions for the transformation of linearly polarized wave into circularly polarized wave.

In order to verify the performance of converting linear-to-circular polarization wave and intuitively represent that circular-polarized wave can be generated, AR is used to indicate the degree of circular polarization of circular-polarized wave. AR is usually obtained by Eq. (5) [27].

$$AR = \frac{\sqrt{r_{xy}^2 + r_{yy}^2 + \sqrt{r_{xy}^4 + r_{yy}^4 + 2r_{xy}^2 r_{yy}^2 \cos(2\Delta\phi)}}}{\sqrt{r_{xy}^2 + r_{yy}^2 - \sqrt{r_{xy}^4 + r_{yy}^4 + 2r_{xy}^2 r_{yy}^2 \cos(2\Delta\phi)}}} \quad (5)$$

Here, r_{xy} is E_x in the reflected wave, and r_{yy} is E_y in the reflected wave. After calculation, $AR = 1$, $AR(\text{dB}) = 0$ [10].

Fig. 6 Surface current distribution of the structure with u - and v -polarized wave at different frequencies: a 3.013THz, b 4.344THz, c 7.974THz, d 10.273THz



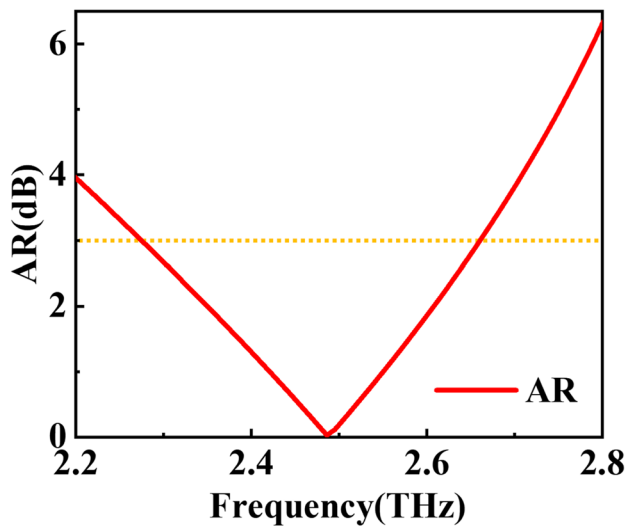


Fig. 8 The axial ratio (AR) of the reflected wave

When $AR = 1$, the reflected wave is a circular-polarized wave. When $AR = \infty$, the reflected wave is a linear-polarized wave. In other cases, the reflected wave is an elliptical-polarized wave. However, unfortunately, no matter the numerical simulation or actual production, sometimes, we are limited by the simulation accuracy, the precision of adaptive mesh, and the process and production tolerance during production, so we cannot get very perfect circular-polarized wave stably. Sometimes, extreme cases including manufacture error may lead to AR more than 3 dB and formation of elliptically polarized reflection wave. Generally, when the AR value is less than 3 dB, the circular-polarized wave effect with better performance can be obtained. In this structure, in the frequency range of 2.28–2.65 THz, it is approximately satisfied the conditions $r_{xy} = r_{yx}$ and $\Delta\phi = 90^\circ$ through simulation and calculation of the structure in the working frequency range. As shown in Fig. 8, it can be seen in 2.28–2.65 THz working frequency that the magnitude of AR is always less than 3 dB; therefore, a better circular-polarized wave has been achieved, which means that it is generally considered that when the calculated axial ratio AR is less than 3 dB, the error from perfect circularly polarized wave is considered to be almost negligible.

Summary

In conclusion, we propose an UWB multifunctional metamaterial structure, composed of the top “I”-shaped resonator, the middle air layer, and the bottom continuous metal plate. The wide bandwidth is attributed to the four electromagnetic resonances generated at the four resonant frequency points of the structure. It is found that the PCR of the proposed the structure reached more than 90% and its relative bandwidth

reached 116% within the frequency range of 2.75–10.35 THz. In addition, this structure achieves linear-to-circular polarization conversion with below 3 dB of AR in the frequency range of 2.28–2.65 THz. The polarization converter proposed in this paper has a simpler geometric structure than the metamaterials proposed in the previous references, but achieves a relatively large relative bandwidth, so this work has many potential applications in radar antenna, metamaterial lens, and other electromagnetic wave and optical fields.

Author Contribution Xiang Miao: conceptualization, methodology, software, writing (original draft), writing (review and editing). Zhongyin Xiao: validation, writing (review and editing), supervision. Zhentao Cui: software, data curation. Tiantian Zheng: software, formal analysis. Xiaoyu Wang: investigation, supervision.

Funding This study is supported by the National Natural Science Foundation of China (grant no. 61275070) and Natural Science Foundation of Shanghai (grant no. 15ZR1415900).

Availability of Data and Materials All data generated or analyzed during this study are included in this published article.

Declarations

Ethics Approval We declare that this article is original, has not been published before, and is not currently considered for publication elsewhere. We confirm that the manuscript has been read and approved by all named authors and that there are no other persons who satisfied the criteria for authorship but are not listed. We further confirm that the order of authors listed in the manuscript has been approved by all of us.

Consent to Participate Written informed consent for participate was obtained from all participants.

Consent for Publication Written informed consent for publication was obtained from all participants.

Competing Interests The authors declare no competing interests.

References

- Beruete M, Navarro-Cia M, Sorolla M, Campillo I (2008) Polarization selection with stacked hole array metamaterial. *J Appl Phys* 103:053102
- Wang Z, Yang Z, Zhao X, Guo L, Guo M (2021) Ultra-wideband and high gain antipodal tapered slot antenna with planar metamaterial lens. *Int J Microw Wirel Technol* 1:11
- de Oliveira JJ, Ribeiro LD, da Silva EJ, de Souza Batalha RM (2021) Design of a free space metamaterial lens based on LC parameters at S-band. *J Electromagn Waves Appl* 35:2210–2223
- Lv F, Xiao Z, Lu X, Chen M (2020) Three-dimensional ultra-broadband metamaterial absorber with full graphite structure. *J Electron Mater* 49:689–694
- Xiao Z, Lv F, Li W, Zou H, Li C (2020) A three-dimensional ultra-broadband and polarization insensitive metamaterial absorber and application for electromagnetic energy harvesting. *Waves in Random and Complex Media* 31(6):2168–2176

6. Chen M, Xiao Z, Lu X, Lv F, Zhou Y (2020) Simulation of dynamically tunable and switchable electromagnetically induced transparency analogue based on metal-graphene hybrid metamaterial. *Carbon* 159:273–282
7. Chen M, Xiao Z, Lv F, Cui Z, Xu Q (2022) Dynamically tunable electromagnetically induced transparency-like effect in terahertz metamaterial based on graphene cross structures. *IEEE J Sel Top Quantum Electron* 28:1–9
8. Chen M, Xiao Z, Lu X, Lv F, Cui Z, Xu Q (2020) Dynamically tunable multi-resonance and polarization-insensitive electromagnetically induced transparency-like based on vanadium dioxide film. *Opt Mater* 102:109811
9. Chen M, Xiao Z, Lv F, Cui Z, Xu Q (2020) Dynamically tunable dual-band electromagnetically induced transparency-like in terahertz metamaterial. *Opt Mater* 107:110060
10. Xu J, Li R, Wang S, Han T (2018) Ultra-broadband linear polarization converter based on anisotropic metasurface. *Opt Express* 26:26235–26241
11. Cui Z, Xiao Z, Chen M, Lv F, Xu Q (2021) A transmissive linear polarization and circular polarization cross polarization converter based on all-dielectric metasurface. *J Electron Mater* 50:4207–4214
12. Zhang H, Yang C, Liu M, Zhang Y (2021) Dual-function tuneable asymmetric transmission and polarization converter in terahertz region. *Res Phys* 25:104242
13. Wang S, Bi J, Liu W, Wen G, Gao S (2021) Polarization-insensitive cross-polarization converter. *IEEE Trans Antennas Propag* 69(8):4670–4680
14. Mei Z, Ma X, Lu C, Zhao Y (2017) High-efficiency and wide-bandwidth linear polarization converter based on double U-shaped metasurface. *AIP Adv* 7:125323
15. Zhao J, Cheng Z (2017) Ultra-broadband and high-efficiency reflective linear polarization converter based on planar anisotropic metamaterial in microwave region. *Optik (Stuttg)* 136:52–57
16. Kamal B, Chen J, Yin Y, Ren J, Ullah S, Ali U (2021) Design and experimental analysis of dual-band polarization converting metasurface. *IEEE Antennas Wirel Propag Lett* 20:3083334
17. Yuan L, Hou L, Zhang Z (2021) Triple-band highly efficient multi-polarization converter based on reflective metasurface. *Prog Electromagn Res M* 102:127–135
18. Qi Y, Zhang B, Liu C, Deng X (2020) Ultra-broadband polarization conversion meta-surface and its application in polarization converter and RCS reduction. *IEEE Access* 8:116675–116684
19. Li S, Cao X, Xu L, Zhou L, Yang H, Han J, Zhang Z, Zhang D, Liu X, Zhang C, Zheng Y, Zhao Y (2016) Ultra-broadband reflective metamaterial with RCS reduction based on polarization converter. *Information Entropy Theory and Genetic Optimization Algorithm*. *Sci Rep* 6:37409
20. Jia Y, Liu Y, Zhang W, Gong S (2016) Ultra-wideband and high-efficiency polarization rotator based on metasurface. *Appl Phys Lett* 109:051901
21. Chen J, Hu Z, Wang G, Huang X, Wang S, Hu X, Liu M (2015) High-impedance surface-based broadband absorbers with interference theory. *IEEE Trans Antennas Propag* 63(10):4367–4374
22. Xiao Z, Zou H, Zheng X, Ling X, Wang L (2017) A tunable reflective polarization converter based on hybrid metamaterial. *Opt Quant Electron* 49:401
23. Zhang X, Ye H, Zhao Y, Zhang H (2021) A tunable ultra-wideband cross-polarization conversion based on the band splicing technology. *Appl Phys B* 127:69
24. Jing X, Gui X, Zhou P, Hong Z (2018) Physical explanation of Fabry-Pérot cavity for broadband bilayer metamaterials polarization converter. *J Lightwave Technol* 36:2322–2327
25. Grady NK, Heyes JE, Chowdhury DR, Zeng Y, Reiten MT, Azad AK, Taylor AJ, Dalvit DAR, Chen H (2013) Terahertz metamaterials for linear polarization conversion and anomalous refraction. *Science* 340:1304–1307
26. Lin B, Guo J, Lv L, Wu J, Ma Y, Liu B, Wang Z (2019) Ultra-wideband and high-efficiency reflective polarization converter for both linear and circular polarized waves. *Appl Phys A* 125:76
27. Lin B, Lv L, Guo J, Liu Z, Ji X, Wu J (2020) An ultra-wideband reflective linear-to-circular polarization converter based on anisotropic metasurface. *IEEE Access* 8:82732–82740

Publisher's Note Springer Nature remains neutral with regard to jurisdictional claims in published maps and institutional affiliations.